Raman spectroscopy and lattice dynamical calculations of Sc_2O_3 single crystals

N. D. Todorov,[1,*] M. V. Abrashev,[1] V. Marinova,[2] M. Kadiyski,[3] L. Dimowa,[3] and E. Faulques[4]
[1]*Faculty of Physics, University of Sofia, BG-1164 Sofia, Bulgaria*
[2]*Institute for Optical Materials and Technologies, Bulgarian Academy of Sciences, BG-1113 Sofia, Bulgaria*
[3]*Institute for Mineralogy and Crystallography, Bulgarian Academy of Sciences, BG-1113 Sofia, Bulgaria*
[4]*Institut des Materiaux Jean Rouxel, Université de Nantes, CNRS, UMR 6502, 2, rue de la Houssiniere, BP 32229, 44322 Nantes, France*
(Received 28 November 2012; published 4 March 2013)

Single crystals of Sc_2O_3 were grown by a high-temperature solution-growth method. They were studied by x-ray single-crystal diffractometry and micro-Raman spectroscopy. In the polarized Raman spectra collected at room temperature all $4A_g + 4E_g$ and 11 out of 14 F_g Raman allowed lines were observed. The vibrational assignment was made by a comparison of the experimentally observed frequencies with calculated ones determined by density functional theory lattice-dynamical calculations.

DOI: 10.1103/PhysRevB.87.104301 PACS number(s): 78.30.Hv, 63.20.D−, 63.20.dk

The rare-earth sesquioxides R_2O_3 are of interest for many different technological applications. With their specific catalytic, magnetic, and electronic properties they appear to be suitable for cathodoluminescence,[1,2] phase stabilizers for solid oxide fuel cells,[3] active catalysts for a large number of organic reactions,[4,5] and high-k gate dielectrics.[6,7] At ambient pressure, depending on the cation radius and temperature, three distinct polymorphic modifications have been identified.[8,9] These crystalline types are labeled as A-type—hexagonal, $P\bar{3}m1$, B-type—monoclinic, $C2/m$, and C-type—cubic, $Ia\bar{3}$, structures, respectively. Sharing similar properties, Sc_2O_3 is considered as a C-type rare-earth sesquioxide and can be used as an excellent host material for high power lasers applications.[3,10–12]

In this paper we report results of a Raman scattering study of large Sc_2O_3 single crystals supported by *ab initio* lattice dynamical calculations (LDC).

Crystals of Sc_2O_3 were grown by a high temperature solution growth method in a Pt crucible. We used Sc_2O_3 powder of 99.995% purity and PbF_2 and NaF of 99.999% purity as starting materials. The ratio of the PbF_2 and NaF solvents was 1:1, while the Sc_2O_3: solvents ratio was 1:10. About 500 g of this mixture are closed in the covered crucible in order to prevent the evaporation of PbF_2, which has high vapor pressure at the growth temperature. The temperature was increased at a rate of 50 °C/h to 1200 °C. To completely dissolve the components of the materials and to achieve a homogeneous solution, the temperature of 1200 °C was maintained for 24 h and then lowered at a rate of 0.5 °C/h to 900 °C. At this temperature the crucible was taken out of the oven, the cover was drilled through, and the solvent is poured out. The obtained crystals remained on the bottom and walls of the crucible.

The crystallographic characterization of the crystal was carried out by x-ray single-crystal diffractometry. A single crystal was mounted on a glass capillary and diffraction data were collected at room temperature by an ω-scan technique, on an Agilent Diffraction SuperNova dual four-circle diffractometer equipped with an Atlas CCD detector. A mirror-monochromatized Mo K_α radiation from a microfocus source was used ($\lambda = 0.7107$ Å). The determination of the cell parameters, data integration, scaling, and absorption correction were carried out using the CRYSALISPRO program package.[13] The structure was solved by direct methods (SHELXS-97)[14] and refined by full-matrix least-square procedures on F^2. The results are listed in Table I. They are in excellent agreement with the previously published data.[15]

The Raman measurements were carried out using micro-Raman spectrometer LabRAM HR800 Visible. At room temperature an objective ×50 was used both to focus the incident laser beam and to collect the scattered light. To check the presence of resonance effects in the Raman spectra, He-Ne (633 nm) and Ar^+ (515, 488, and 458 nm) lasers were used as excitation sources.

First-principles calculations were performed with the CASTEP[16] code, using density functional perturbational theory (DFPT) within the local density approximation (LDA). Norm-conserving pseudopotentials were generated by the optimized approach[17] with the following atomic valence configurations: O ($2s^2 2p^4$) and Sc ($3s^2 3p^6 3d^1 4s^2$). Brillouin zone summations were carried out with a $2 \times 2 \times 2$ Monkhorst-Pack k-point mesh. The calculated LDA lattice parameters are slightly underestimated, but the agreement with the experimental data is better than 0.3%.

The C-type crystal structure of Sc_2O_3 can be described as an oxygen-deficient superstructure of the simpler CeO_2 (CaF_2-type crystal structure) if each fourth oxygen atom from the oxygen chains parallel to all {100} crystal directions is removed (see Fig. 1). This reduces the oxygen environment of the Sc atoms from eight (in the CaF_2-type structure) to six atoms by distributing them onto two different Wyckoff positions (8b and 24d, see Table I). The Sc atoms at 8b positions have a sixfold oxygen environment, resulting after the removal of two oxygen atoms, lying on the [111] cubic body diagonal. The Sc atoms at 24d positions have a sixfold oxygen environment because of the removal of two oxygen atoms, lying on the [110] cubic face diagonal (see Fig. 2). The resulting body-centered $Ia\bar{3}$ cubic unit cell (with a volume eight times larger than that of the unit cell of the parent CeO_2) contains 16 formula units. The irreducible representations of the Γ-point phonon modes are $\Gamma_{\text{Total}} = 4A_g + 5A_u + 4E_g + 5E_u + 14F_g + 17F_u$ (see Table II). The Raman-active modes

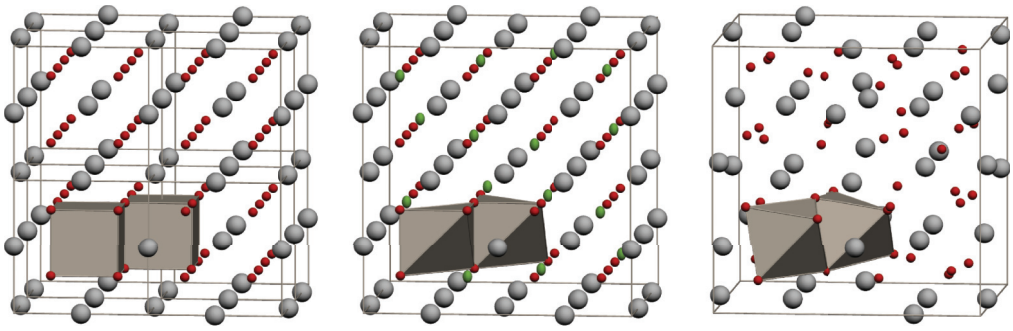

FIG. 1. (Color online) (a) The crystal structure of CeO_2 (CaF_2-type) $2 \times 2 \times 2$ super cell. The eightfold cubic oxygen environment of the two adjacent Ce atoms is given. (b) Hypothetical oxygen-deficient superstructure of CeO_{2-x} ($x = 0.5$), the vacancies are represented by the green ellipsoids. (c) The real structure of Sc_2O_3.

are $\Gamma_{\text{Raman}} = 4A_g + 4E_g + 14F_g$ with the following Raman tensors:[18]

$$A_g = \begin{pmatrix} a & 0 & 0 \\ 0 & a & 0 \\ 0 & 0 & a \end{pmatrix},$$

$$E_g^{(1)} = \begin{pmatrix} b+\sqrt{3}c & 0 & 0 \\ 0 & b-\sqrt{3}c & 0 \\ 0 & 0 & -2b \end{pmatrix},$$

$$E_g^{(2)} = \begin{pmatrix} c-\sqrt{3}b & 0 & 0 \\ 0 & c+\sqrt{3}b & 0 \\ 0 & 0 & -2c \end{pmatrix},$$

$$F_g^{(1)} = \begin{pmatrix} 0 & 0 & 0 \\ 0 & 0 & d \\ 0 & d & 0 \end{pmatrix},$$

$$F_g^{(2)} = \begin{pmatrix} 0 & 0 & d \\ 0 & 0 & 0 \\ d & 0 & 0 \end{pmatrix},$$

$$F_g^{(3)} = \begin{pmatrix} 0 & d & 0 \\ d & 0 & 0 \\ 0 & 0 & 0 \end{pmatrix}.$$

The symmetry of the lines in the Raman spectra can be easily determined comparing the intensity of the lines in four types of spectra, obtained in different scattering configurations, see Table III. (x, y) and (x', y') are two pairs of perpendicular directions, parallel to {100} and {110} crystal directions, respectively (see Fig. 3).

The studied single crystal is shown in Fig. 3. Its longest edges are parallel to {100} crystal directions. The polarized Raman spectra, obtained in the appropriate scattering configurations, mentioned above, are shown in Fig. 4. The comparison of the spectra, obtained with different excitation wavelength, shows that the relative intensity of the lines in spectra in a given scattering configuration remains nearly the same. This proves their Raman origin and shows that the resonance effects are negligible. The lines, originated by a leakage of about 5% (caused by the scattered light analyzer) and forbidden for the given geometrical configuration, are marked with filled circles. In the spectra obtained with 633 nm He-Ne line (not shown here), a relatively strong background, rapidly increasing at higher frequencies, was observed. Its origin can be related to the presence of Cr atoms with concentration about 10^{-4} in the Sc_2O_3 crystal, which were added to check the properties of the material for laser applications.

TABLE I. Structural data of Sc_2O_3. Space group No. 206 ($Ia\bar{3}$), $Z = 16$, $a = 9.8300$ Å.

Atom	Valence	Wyckoff notation	x	y	z
Sc1	+3	8b	1/4	1/4	1/4
Sc2	+3	24d	0.46456	0	1/4
O	−2	48e	0.39127	0.15470	0.38155

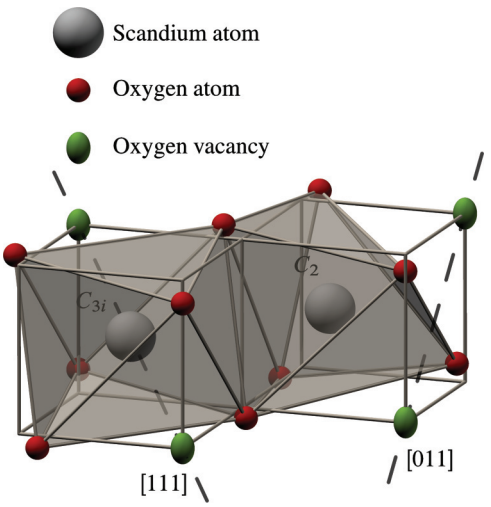

FIG. 2. (Color online) Sc atoms occupy two different sets of atomic positions 8*b* and 24*d* corresponding to C_{3i} and C_2 site symmetry, and the oxygen atoms are on general position 48*e* with C_1 site symmetry.

TABLE II. Wyckoff position of the atoms in the unit cell of Sc_2O_3. The irreducible representations of the Γ-point phonon modes are $\Gamma_{\text{Total}} = 4A_g + 5A_u + 4E_g + 5E_u + 14F_g + 17F_u$ (Ref. 18).

Atom	Wyckoff notation	Irreducible representation
Sc1	8b	$A_u + E_u + 3F_u$
Sc2	24d	$A_g + A_u + E_g + E_u + 5F_g + 5F_u$
O	48e	$3A_g + 3A_u + 3E_g + 3E_u + 9F_g + 9F_u$

From Fig. 4 and Table III the symmetry of the following intense lines can be immediately determined: 221 and 495 cm^{-1}—A_g; 273 and 430 cm^{-1}—E_g; 189, 319, 419, and 523 cm^{-1}—F_g. The weak lines at 202, 252, 329, 587, and 669 cm^{-1} also have F_g symmetry. After careful decomposition of the profile of the lines near 359, 391, and 623–626 cm^{-1} in the different types of spectra, it was found that the line near 359 cm^{-1} consists of two lines with E_g and F_g symmetry, the line near 391 cm^{-1} consists of two lines with A_g and F_g symmetry, and the line near 623–626 cm^{-1} consists of two lines with A_g (623 cm^{-1}) and E_g (626 cm^{-1}) symmetry. The frequencies and the symmetry of all lines observed are tabulated in Table IV. It can be seen that experimentally observed and calculated frequencies of all A_g and E_g modes are very close. Moreover, comparing the relative intensity of the experimentally observed lines with the calculated Raman spectrum for $z(yx)\bar{z}$ (where only modes with F_g symmetry are allowed), one finds that the relative intensity of the corresponding lines in the two spectra are very close (for better comparison the calculated lines are presented as Lorentzians with linewidth, fixed at $\Gamma = 3.5$ cm^{-1}, see Fig. 5). Therefore, we can assign the 11 observed F_g lines to the F_g modes with closest calculated frequencies. Based on the LDC it appears that the frequencies of the remaining three F_g modes should be close to 365, 444, and 489 cm^{-1}. From LDC we can also conclude that all modes with frequency below 300 cm^{-1} are predominantly vibrations of Sc atoms, whereas those with higher frequency are almost pure oxygen vibrations. This fact can be used for future identification of the corresponding modes in the isostructural C-type phase R_2O_3 compounds.

We have to point out that up to now only nonpolarized Raman spectra, obtained from Sc_2O_3 ceramic or powder samples were published.[19–22] However, although the frequencies of the lines measured in this work are close to those in Refs. 19–21, there is a systematic frequency difference by 13 cm^{-1} with those of Ref. 22. For this reason in Table IV we give for comparison only the frequencies from the first two papers. It also worth mentioning here that due to the very low noise-signal ratio of our Raman spectra we were able to identify lines (e.g., at 202 and 329 cm^{-1}) of intensity about three orders weaker than the intensity of the most intense line (at 419 cm^{-1}). Therefore, the origin of some additional lines, reported in Ref. 19 or Ref. 22 but not observed in our spectra, is questionable.

TABLE III. Selection rules for Raman-active modes for a crystal structure with $Ia\bar{3}$ space group in specific scattering configurations. $e^2 \equiv b^2 + c^2$.

	xx	yx	$x'x'$	$y'x'$
A_g	a^2	0	a^2	0
E_g	$4e^2$	0	e^2	$3e^2$
F_g	0	d^2	d^2	0

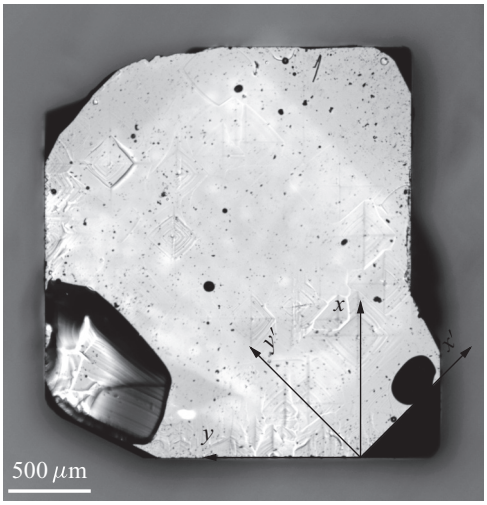

FIG. 3. The studied Sc_2O_3 single crystal. (x, y) and (x', y') are two pairs of perpendicular directions, parallel to {100} and {110} crystal directions, respectively.

TABLE IV. Comparison between the previously published, experimentally observed ($\omega_{\text{expt.}}$), and calculated by CASTEP ($\omega_{\text{calc.}}$) frequencies (in cm^{-1}) of Raman-active modes of Sc_2O_3.

Symmetry	Ref. 19	Ref. 20	$\omega_{\text{expt.}}$	$\omega_{\text{calc.}}$	$\Delta\omega$
A_g	222	222	221	215	6
	392	391	391	395	−4
	495	495	495	478	17
			623	618	5
E_g	274	273	273	269	4
	358	358	359	361	−2
		428	430	434	−4
	628		626	620	6
F_g	190	190	189	180	9
			202	194	8
			252	249	3
	320	320	319	317	2
			329	325	4
		358	359	361	−2
				366	
	392	391	391	386	5
	419	419	419	426	−7
				444	
				489	
	525	524	523	512	11
			587	584	3
	674		669	663	6

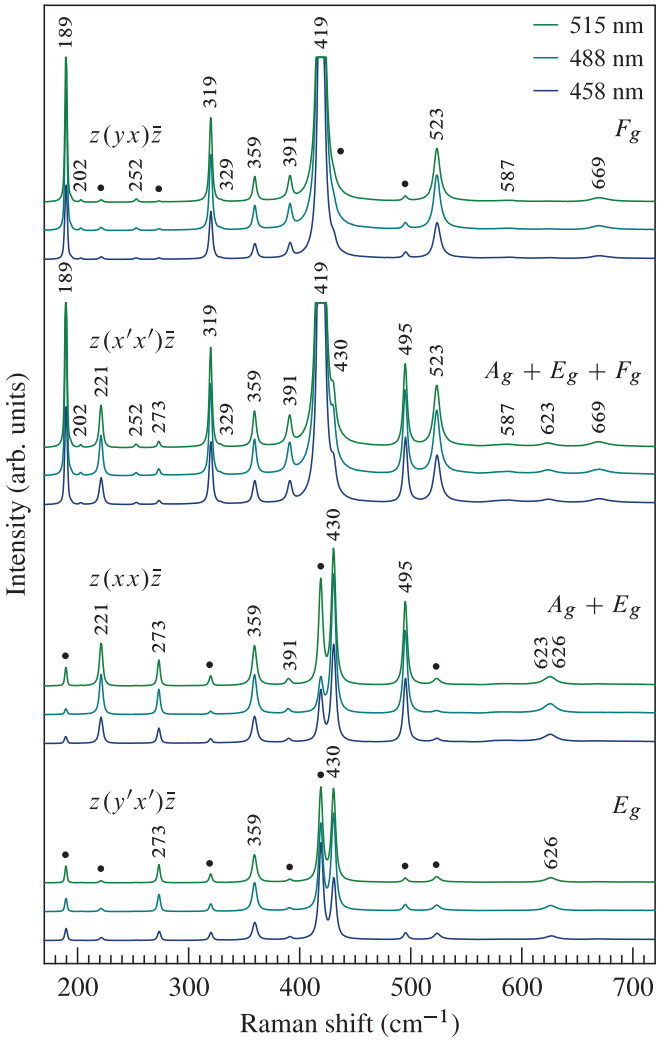

FIG. 4. (Color online) Polarized Raman spectra of Sc_2O_3, collected from (100) surface with $\lambda_L = 515$, 488, and 458 nm excitation at room temperature. The lines, indicated with a wave number (in cm^{-1}), are allowed for the corresponding geometrical configuration. The lines, marked with filled circles, are forbidden for the given configuration. The geometrical configuration of the spectra as well the symmetry of the lines, allowed for it, are also given.

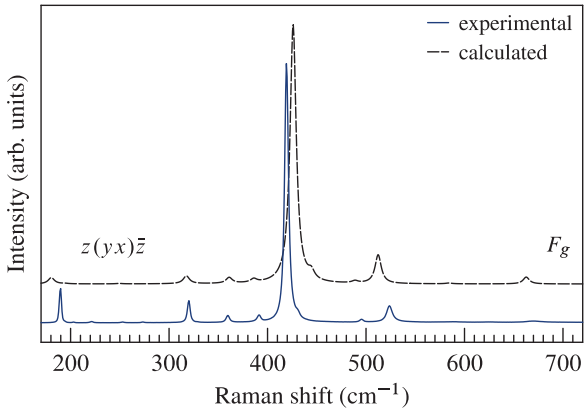

FIG. 5. (Color online) A comparison of the calculated and experimentally measured ($\lambda_L = 488$ nm) $z(yx)\bar{z}$ Raman spectrum (where only modes with F_g symmetry are allowed).

It is worth noting to comment the fact that only one line (F_g at 419 cm^{-1}) has very large intensity compared to the rest. In the parent compound (CeO_2) due to the smaller unit cell and higher symmetry there is only one Raman-active mode F_{2g} (464 cm^{-1}, Refs. 23 and 24). The pattern of this mode can be determined only by symmetry considerations—it is triply degenerated out-of-phase antistretching oxygen vibration along the {100} crystal directions. Our LDC predict that the shape of F_g mode at 419 cm^{-1} in Sc_2O_3 is very close to the F_{2g} one in CeO_2. So, these two modes can be considered as corresponding ones in these two structures.

In summary, we report a complete analysis of Raman data of Sc_2O_3 single crystals, supported by *ab initio* lattice dynamical calculations. The obtained results can be used as a reference data in studies of other C-type sesquoxides.

This work has been supported by the Science Fund of the University of Sofia (Contract No. 67/2012) and by the American Physical Society through an International Travel Grant 2012 (MVA). We also thank Milko Iliev (TcSUH, Houston, TX, USA) and Xavier Rocquefelte (IMN, Nantes, France) for the helpful discussions.

*neno@phys.uni-sofia.bg

[1] E. W. Barrera, M. C. Pujol, F. Diaz, S. B. Choi, F. Rotermund, K. H. Park, M. S. Jeong, and C. Cascales, Nanotechnology **22**, 075205 (2011).
[2] A. H. Kitai, Thin Solid Films **445**, 367 (2003).
[3] N. Orlovskaya, S. Lukich, G. Subhash, T. Graule, and J. Kuebler, J. Power Sources **195**, 2774 (2010).
[4] G. A. Hussein, J. Analyt. Appl. Pyroly. **37**, 111 (1996).
[5] A. Dedov, A. Loktev, I. Moiseev, A. Aboukais, J.-F. Lamonier, and I. Filimonov, Appl. Cataly. A: General **245**, 209 (2003).
[6] E. Miranda, J. Molina, Y. Kim, and H. Iwai, Microelectron. Reliability **45**, 1365 (2005).
[7] T.-M. Pan and W.-S. Huang, Appl. Surf. Sci. **255**, 4979 (2009).
[8] M. Zinkevich, Prog. Mater. Sci. **52**, 597 (2007).
[9] M. Rahm and N. V. Skorodumova, Phys. Rev. B **80**, 104105 (2009).
[10] R. Peters, C. Krnkel, K. Petermann, and G. Huber, Opt. Express **15**, 7075 (2007).
[11] J. Lu, J. F. Bisson, K. Takaichi, T. Uematsu, A. Shirakawa, M. Musha, K. Ueda, H. Yagi, T. Yanagitani, and A. A. Kaminskii, Appl. Phys. Lett. **83**, 1101 (2003).
[12] A. Shirakawa, K. Takaichi, H. Yagi, J. Bisson, J. L. M. Musha, K. Ueda, T. Yanagitani, T. Petrov, and A. Kaminskii, Opt. Express **11**, 2911 (2003).
[13] CRYSALISPRO, Agilent Technologies UK Ltd., 2010.
[14] G. M. Sheldrick, Acta Crystallogr. Sect. A **64**, 112 (2008).
[15] C. H. Jiang, Z. H. Jin, Y. Bin, Y. W. Tao, Z. Xian, W. J. Yang, and Z. G. Cai, Crystal Growth Design **10**, 4389 (2010).

[16]S. J. Clark, M. D. Segall, C. J. Pickard, P. J. Hasnip, M. I. J. Probert, K. Refson, and M. C. Payne, Z. Kristallogr. **220**, 567 (2005).

[17]A. M. Rappe, K. M. Rabe, E. Kaxiras, and J. D. Joannopoulos, Phys. Rev. B **41**, 1227 (1990).

[18]E. Kroumova, M. I. Aroyo, J. M. Perez-Mato, A. Kirov, C. Capillas, S. Ivantchev, and H. Wondratschek, Phase Transit. **76**, 155 (2003); M. I. Aroyo, A. Kirov, C. Capillas, J. M. Perez-Mato, and H. Wondratschek, Acta Crystallogr. Sect. A **62**, 115 (2006); M. I. Aroyo, J. M. Perez-Mato, C. Capillas, E. Kroumova, S. Ivantchev, G. Madariaga, A. Kirov, and H. Wondratschek, Z. Kristallogr. **221**, 15 (2006).

[19]D. Liu, W. Lei, Y. Li, Y. Ma, J. Hao, X. Chen, Y. Jin, D. Liu, S. Yu, Q. Cui, and G. Zou, Inorg. Chem. **48**, 8251 (2009).

[20]A. A. Kaminskii, S. N. Bagaev, K. Ueda, K. Takaichi, J. Lu, A. Shirakawa, H. Yagi, T. Yanagitani, H. J. Eichler, and H. Rhee, Laser Phys. Lett. **2**, 30 (2005).

[21]A. Ubaldini and M. M. Carnasciali, J. Alloys Compd. **454**, 374 (2008).

[22]W. B. White and V. G. Keramidas, Spectrochim. Acta Part A **28**, 501 (1972).

[23]T. Sato and S. Tateyama, Phys. Rev. B **26**, 2257 (1982).

[24]G. A. Kourouklis, A. Jayaraman, and G. P. Espinosa, Phys. Rev. B **37**, 4250 (1988).